Decoupling Properties of the Cubic Architecture

Thomas Dehaeze[1]
ESRF, The European Synchrotron
Grenoble, France
email: thomas.dehaeze@esrf.fr

Christophe Collette
Precision Mechatronics Laboratory
University of Liège, Belgium
email: christophe.collette@uliege.be

This is the abstract. This article illustrates preparation of ASME paper using Please use this template to test how your figures will look on the printed journal page of the Journal of Mechanical Design. The Journal will no longer publish papers that contain errors in figure resolution. These usually consist of unreadable or fuzzy text, and pixilation or rasterization of lines. This template identifies the specifications used by JMD some of which may not be easily duplicated; for example, ASME actually uses Helvetica Condensed Bold, but this is not generally available so for the purpose of this exercise Helvetica is adequate. However, reproduction of the journal page is not the goal, instead this exercise is to verify the quality of your figures. Notice that this abstract is to be set in 9pt Times Italic, single spaced and right justified.

1 Introduction

The Cubic configuration for the Stewart platform was first proposed by Dr. Gough in a comment to the original paper by Dr. Stewart [1]. This configuration is characterized by active struts arranged in a mutually orthogonal configuration connecting the corners of a cube, as shown in Figure 1(*a*).

Typically, the struts have similar length to the cube's edges, as illustrated in Figure 1(*a*). Practical implementations of such configurations can be observed in Figures **??**, **??** and **??**. It is also possible to implement designs with strut lengths smaller than the cube's edges (Figure 1(*b*)), as exemplified in Figure **??**.

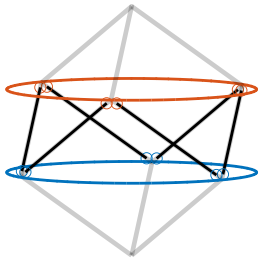

(*a*) Classical Cubic architecture

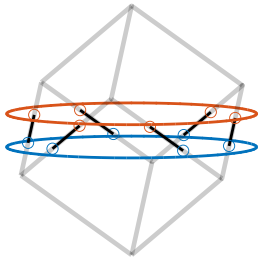

(*b*) Alternative configuration

Figure 1 Typical Stewart platform cubic architectures in which struts' length is similar to the cube edges's length ((*a*)) or is taking just a portion of the edge ((*b*)).

Several advantageous properties attributed to the cubic configuration have contributed to its widespread adoption [2–4]: simplified kinematics relationships and dynamical analysis [2]; uniform stiffness in all directions [5]; uniform mobility [6, , chapt.8.5.2]; and minimization of the cross coupling between actuators and sensors in different struts [3]. This minimization is attributed to the fact that the struts are orthogonal to each other, and is said to facilitate collocated sensor-actuator control system design, i.e., the implementation of decentralized control [2,7].

These properties are examined in this section to assess their relevance for the nano-hexapod. The mobility and stiffness properties of the cubic configuration are analyzed in Section 2. Dynamical decoupling is investigated in Section 3, while decentralized control, crucial for the NASS, is examined in Section 4. Given that the cubic architecture imposes strict geometric constraints, alternative designs are proposed in Section 5. The ultimate objective is to determine the suitability of the cubic architecture for the nano-hexapod.

2 Static Properties

2.1 Stiffness matrix for the Cubic architecture. Consider the cubic architecture shown in Figure 2(*a*). The unit vectors corresponding to the edges of the cube are described by equation (1).

$$\hat{s}_1 = \begin{bmatrix} \frac{\sqrt{2}}{\sqrt{3}} \\ 0 \\ \frac{1}{\sqrt{3}} \end{bmatrix} \quad \hat{s}_2 = \begin{bmatrix} \frac{-1}{\sqrt{6}} \\ \frac{-1}{\sqrt{2}} \\ \frac{1}{\sqrt{3}} \end{bmatrix} \quad \hat{s}_3 = \begin{bmatrix} \frac{-1}{\sqrt{6}} \\ \frac{1}{\sqrt{2}} \\ \frac{1}{\sqrt{3}} \end{bmatrix}$$
$$\hat{s}_4 = \begin{bmatrix} \frac{\sqrt{2}}{\sqrt{3}} \\ 0 \\ \frac{1}{\sqrt{3}} \end{bmatrix} \quad \hat{s}_5 = \begin{bmatrix} \frac{-1}{\sqrt{6}} \\ \frac{-1}{\sqrt{2}} \\ \frac{1}{\sqrt{3}} \end{bmatrix} \quad \hat{s}_6 = \begin{bmatrix} \frac{-1}{\sqrt{6}} \\ \frac{1}{\sqrt{2}} \\ \frac{1}{\sqrt{3}} \end{bmatrix} \tag{1}$$

Coordinates of the cube's vertices relevant for the top joints, expressed with respect to the cube's center, are shown in equation (2).

$$\tilde{\boldsymbol{b}}_1 = \tilde{\boldsymbol{b}}_2 = H_c \begin{bmatrix} \frac{1}{\sqrt{2}} \\ \frac{-\sqrt{3}}{\sqrt{2}} \\ \frac{1}{2} \end{bmatrix}, \quad \tilde{\boldsymbol{b}}_3 = \tilde{\boldsymbol{b}}_4 = H_c \begin{bmatrix} \frac{1}{\sqrt{2}} \\ \frac{\sqrt{3}}{\sqrt{2}} \\ \frac{1}{2} \end{bmatrix},$$
$$\tilde{\boldsymbol{b}}_5 = \tilde{\boldsymbol{b}}_6 = H_c \begin{bmatrix} \frac{-2}{\sqrt{2}} \\ 0 \\ \frac{1}{2} \end{bmatrix} \tag{2}$$

In the case where top joints are positioned at the cube's vertices, a diagonal stiffness matrix is obtained as shown in equation (3). Translation stiffness is twice the stiffness of the struts, and

[1] Corresponding Author.
Version 1.26, November 27, 2025

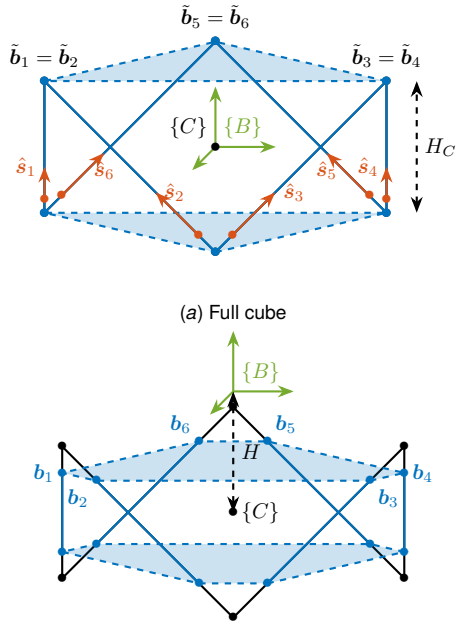

Figure 2 Cubic architecture. Struts are represented in blue. The cube's center by a black dot. The Struts can match the cube's edges ((*a*)) or just take a portion of the edge ((*b*))

rotational stiffness is proportional to the square of the cube's size H_c.

$$\boldsymbol{K} = k \begin{bmatrix} 2 & 0 & 0 & 0 & 0 & 0 \\ 0 & 2 & 0 & 0 & 0 & 0 \\ 0 & 0 & 2 & 0 & 0 & 0 \\ 0 & 0 & 0 & \frac{3}{2}H_c^2 & 0 & 0 \\ 0 & 0 & 0 & 0 & \frac{3}{2}H_c^2 & 0 \\ 0 & 0 & 0 & 0 & 0 & 6H_c^2 \end{bmatrix} \tag{3}$$

However, typically, the top joints are not placed at the cube's vertices but at positions along the cube's edges (Figure 2(*b*)). In that case, the location of the top joints can be expressed by equation (4), yet the computed stiffness matrix remains identical to Equation (3).

$$\boldsymbol{b}_i = \tilde{\boldsymbol{b}}_i + \alpha \hat{\boldsymbol{s}}_i \tag{4}$$

The stiffness matrix is therefore diagonal when the considered $\{B\}$ frame is located at the center of the cube (shown by frame $\{C\}$). This means that static forces (resp torques) applied at the cube's center will induce pure translations (resp rotations around the cube's center). This specific location where the stiffness matrix is diagonal is referred to as the "Center of Stiffness" (analogous to the "Center of Mass" where the mass matrix is diagonal).

2.2 Effect of having frame $\{B\}$ off-centered. When the reference frames $\{A\}$ and $\{B\}$ are shifted from the cube's center, off-diagonal elements emerge in the stiffness matrix.

Considering a vertical shift as shown in Figure 2(*b*), the stiffness matrix transforms into that shown in Equation (5). Off-diagonal elements increase proportionally with the height difference between the cube's center and the considered $\{B\}$ frame.

$$\boldsymbol{K} = k \begin{bmatrix} 2 & 0 & 0 & 0 & -2H & 0 \\ 0 & 2 & 0 & 2H & 0 & 0 \\ 0 & 0 & 2 & 0 & 0 & 0 \\ 0 & 2H & 0 & \frac{3}{2}H_c^2 + 2H^2 & 0 & 0 \\ -2H & 0 & 0 & 0 & \frac{3}{2}H_c^2 + 2H^2 & 0 \\ 0 & 0 & 0 & 0 & 0 & 6H_c^2 \end{bmatrix} \tag{5}$$

This stiffness matrix structure is characteristic of Stewart platforms exhibiting symmetry, and is not an exclusive property of cubic architectures. Therefore, the stiffness characteristics of the cubic architecture are only distinctive when considering a reference frame located at the cube's center. This poses a practical limitation, as in most applications, the relevant frame (where motion is of interest and forces are applied) is located above the top platform.

It should be noted that for the stiffness matrix to be diagonal, the cube's center doesn't need to coincide with the geometric center of the Stewart platform. This observation leads to the interesting alternative architectures presented in Section 5.

2.3 Uniform Mobility. The translational mobility of the Stewart platform with constant orientation was analyzed. Considering limited actuator stroke (elongation of each strut), the maximum achievable positions in XYZ space were estimated. The resulting mobility in X, Y, and Z directions for the cubic architecture is illustrated in Figure 3(*a*).

The translational workspace analysis reveals that for the cubic architecture, the achievable positions form a cube whose axes align with the struts, with the cube's edge length corresponding to the strut axial stroke. These findings suggest that the mobility pattern is more subtle than sometimes described in the literature [8], exhibiting uniformity primarily along directions aligned with the cube's edges rather than uniform spherical distribution in all XYZ directions. This configuration still offers more consistent mobility characteristics compared to alternative architectures illustrated in Figure **??**.

The rotational mobility, illustrated in Figure 3(*b*), exhibits greater achievable angular stroke in the R_x and R_y directions compared to the R_z direction. Furthermore, an inverse relationship exists between the cube's dimension and rotational mobility, with larger cube sizes corresponding to more limited angular displacement capabilities.

3 Dynamical Decoupling

This section examines the dynamics of the cubic architecture in the Cartesian frame which corresponds to the transfer function from forces and torques $\mathcal{F}$ to translations and rotations $\mathcal{X}$ of the top platform. When relative motion sensors are integrated in each strut (measuring $\mathcal{L}$), the pose $\mathcal{X}$ is computed using the Jacobian matrix as shown in Figure 4.

3.1 Low frequency and High frequency coupling. As derived during the conceptual design phase, the dynamics from $\mathcal{F}$ to $\mathcal{X}$ is described by Equation (**??**). At low frequency, the behavior of the platform depends on the stiffness matrix (6).

$$\frac{\mathcal{X}}{\mathcal{F}}(j\omega) \xrightarrow[\omega \to 0]{} \boldsymbol{K}^{-1} \tag{6}$$

In Section 2, it was demonstrated that for the cubic configuration, the stiffness matrix is diagonal if frame $\{B\}$ is positioned at the cube's center. In this case, the "Cartesian" plant is decoupled at low frequency. At high frequency, the behavior is governed by the mass matrix (evaluated at frame $\{B\}$) (7).

$$\frac{\mathcal{X}}{\mathcal{F}}(j\omega) \xrightarrow[\omega \to \infty]{} -\omega^2 \boldsymbol{M}^{-1} \tag{7}$$

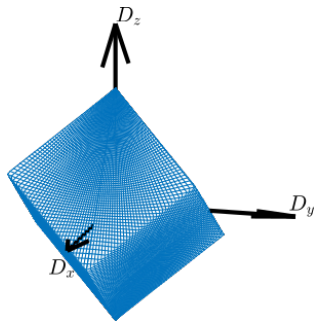

(*a*) Mobility in translation

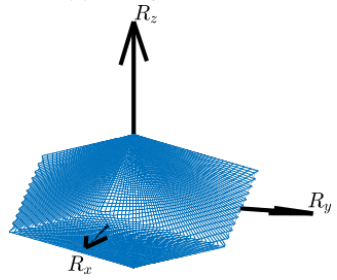

(*b*) Mobility in rotation

Figure 3 Mobility of a Stewart platform with Cubic architecture. Both for translations ((*a*)) and rotations ((*b*))

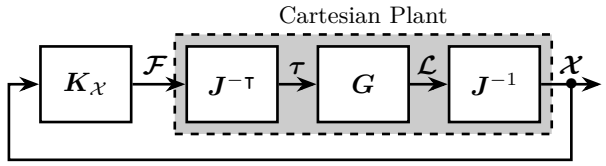

Figure 4 Typical control architecture in the cartesian frame

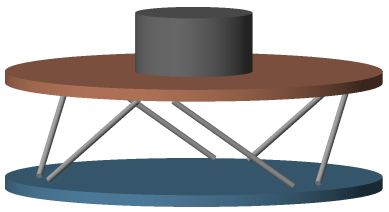

Figure 5 Cubic stewart platform with top cylindrical payload

To achieve a diagonal mass matrix, the center of mass of the mobile components must coincide with the $\{B\}$ frame, and the principal axes of inertia must align with the axes of the $\{B\}$ frame.

To verify these properties, a cubic Stewart platform with a cylindrical payload was analyzed (Figure 5). Transfer functions from $\mathcal{F}$ to $\mathcal{X}$ were computed for two specific locations of the $\{B\}$ frames. When the $\{B\}$ frame was positioned at the center of mass, coupling at low frequency was observed due to the non-diagonal stiffness matrix (Figure 6(*a*)). Conversely, when positioned at the center of stiffness, coupling occurred at high frequency due to the non-diagonal mass matrix (Figure 6(*b*)).

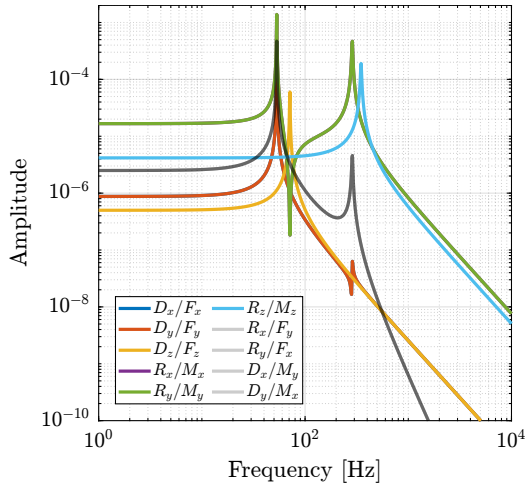

(*a*) $\{B\}$ at the center of mass

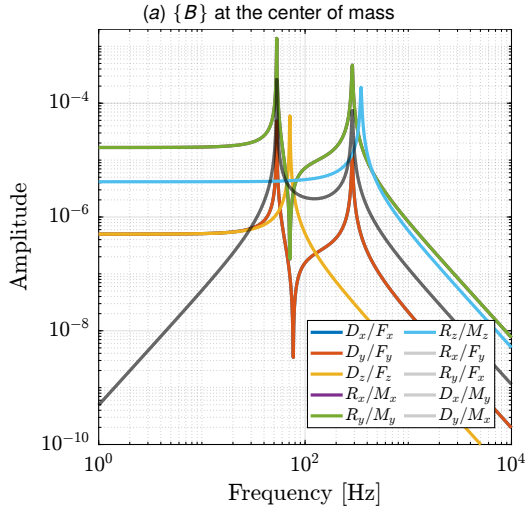

(*b*) $\{B\}$ at the cube's center

Figure 6 Transfer functions for a Cubic Stewart platform expressed in the Cartesian frame. Two locations of the $\{B\}$ frame are considered: at the center of mass of the moving body ((*a*)) and at the cube's center ((*b*)).

3.2 Payload's CoM at the cube's center. An effective strategy for improving dynamical performances involves aligning the cube's center (center of stiffness) with the center of mass of the moving components [9]. This can be achieved by positioning the payload below the top platform, such that the center of mass of the moving body coincides with the cube's center (Figure 7(*a*)). This approach was physically implemented in several studies [4,10]. The resulting dynamics are indeed well-decoupled (Figure 7(*b*)), taking advantage from diagonal stiffness and mass matrices. The primary limitation of this approach is that, for many applications

including the nano-hexapod, the payload must be positioned above the top platform. If a design similar to Figure 7(*a*) were employed for the nano-hexapod, the X-ray beam would intersect with the struts during spindle rotation.

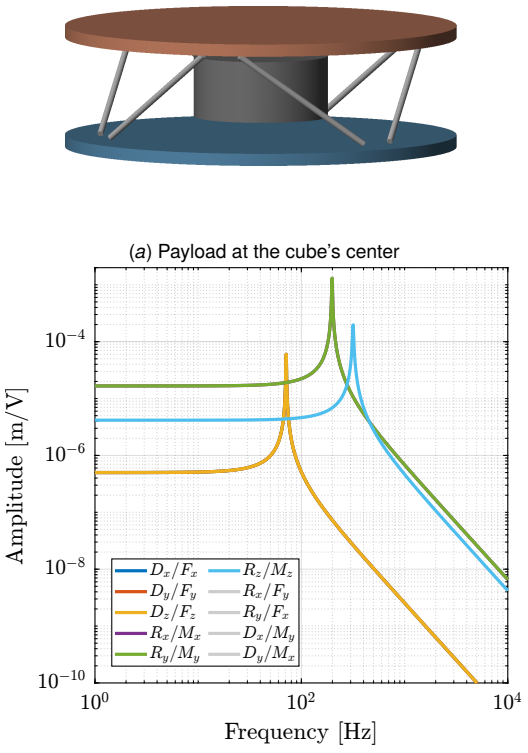

Figure 7 Cubic Stewart platform with payload at the cube's center ((*a*)). Obtained cartesian plant is fully decoupled ((*b*))

3.3 Conclusion. The analysis of dynamical properties of the cubic architecture yields several important conclusions. Static decoupling, characterized by a diagonal stiffness matrix, is achieved when reference frames $\{A\}$ and $\{B\}$ are positioned at the cube's center. Note that this property can also be obtained with non-cubic architectures that exhibit symmetrical strut arrangements. Dynamic decoupling requires both static decoupling and coincidence of the mobile platform's center of mass with reference frame $\{B\}$. While this configuration offers powerful control advantages, it requires positioning the payload at the cube's center, which is highly restrictive and often impractical.

4 Decentralized Control

The orthogonal arrangement of struts in the cubic architecture suggests a potential minimization of inter-strut coupling, which could theoretically create favorable conditions for decentralized control. Two sensor types integrated in the struts are considered: displacement sensors and force sensors. The control architecture is illustrated in Figure 8, where $\boldsymbol{K}_{\mathcal{L}}$ represents a diagonal transfer function matrix.

The obtained plant dynamics in the frame of the struts are compared for two Stewart platforms. The first employs a cubic architecture shown in Figure 5. The second uses a non-cubic Stewart platform shown in Figure 9, featuring identical payload and strut dynamics but with struts oriented more vertically to differentiate it from the cubic architecture.

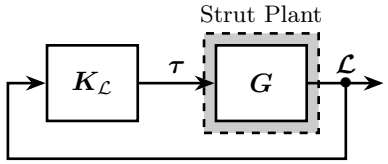

Figure 8 Decentralized control in the frame of the struts.

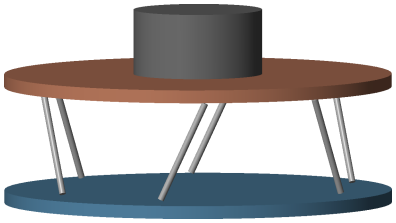

Figure 9 Stewart platform with non-cubic architecture

4.1 Relative Displacement Sensors. The transfer functions from actuator force in each strut to the relative motion of the struts are presented in Figure 10. As anticipated from the equations of motion from $\boldsymbol{f}$ to $\boldsymbol{\mathcal{L}}$ (**??**), the 6×6 plant is decoupled at low frequency. At high frequency, coupling is observed as the mass matrix projected in the strut frame is not diagonal.

No significant advantage is evident for the cubic architecture (Figure 10(*b*)) compared to the non-cubic architecture (Figure 10(*a*)). The resonance frequencies differ between the two cases because the more vertical strut orientation in the non-cubic architecture alters the stiffness properties of the Stewart platform, consequently shifting the frequencies of various modes.

4.2 Force Sensors. Similarly, the transfer functions from actuator force to force sensors in each strut were analyzed for both cubic and non-cubic Stewart platforms. The results are presented in Figure 11. The system demonstrates good decoupling at high frequency in both cases, with no clear advantage for the cubic architecture.

4.3 Conclusion. The presented results do not demonstrate the pronounced decoupling advantages often associated with cubic architectures in the literature. Both the cubic and non-cubic configurations exhibited similar coupling characteristics, suggesting that the benefits of orthogonal strut arrangement for decentralized control is less obvious than often reported in the literature.

5 Cubic architecture with Cube's center above the top platform

As demonstrated in Section 3, the cubic architecture can exhibit advantageous dynamical properties when the center of mass of the moving body coincides with the cube's center, resulting in diagonal mass and stiffness matrices. As shown in Section 2, the stiffness matrix is diagonal when the considered $\{B\}$ frame is located at the cube's center. However, the $\{B\}$ frame is typically positioned above the top platform where forces are applied and displacements are measured.

This section proposes modifications to the cubic architecture to enable positioning the payload above the top platform while still leveraging the advantageous dynamical properties of the cubic configuration.

Three key parameters define the geometry of the cubic Stewart platform: H, the height of the Stewart platform (distance from fixed base to mobile platform); H_c, the height of the cube, as shown in

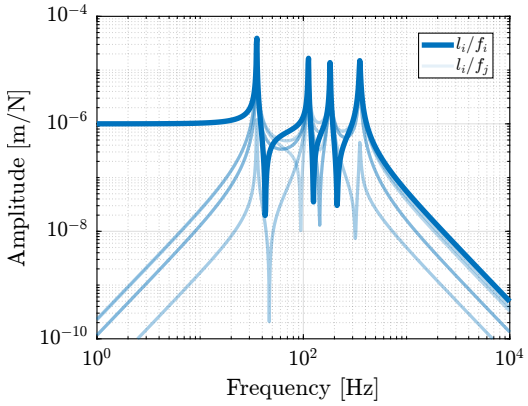

(*a*) Non cubic architecture

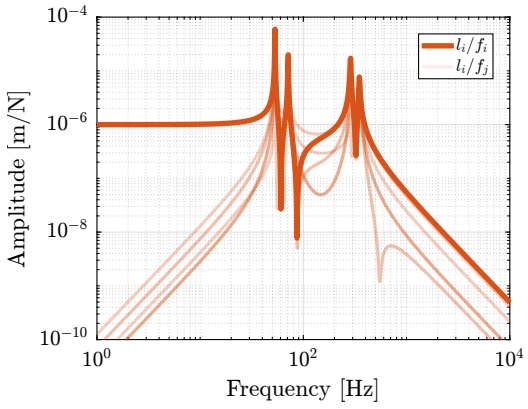

(*b*) Cubic architecture

Figure 10 Bode plot of the transfer functions from actuator force to relative displacement sensor in each strut. Both for a non-cubic architecture ((*a*)) and for a cubic architecture ((*b*))

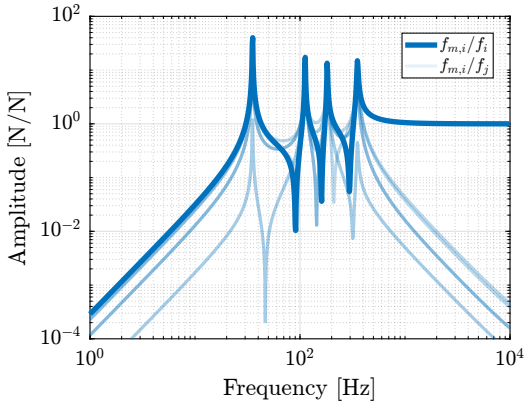

(*a*) Non cubic architecture

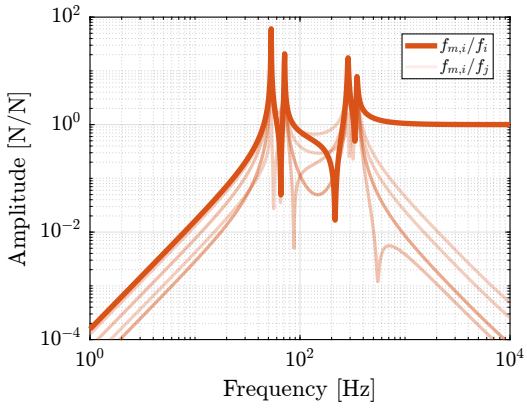

(*b*) Cubic architecture

Figure 11 Bode plot of the transfer functions from actuator force to force sensor in each strut. Both for a non-cubic architecture ((*a*)) and for a cubic architecture ((*b*))

Figure 2(*a*); and H_{CoM}, the height of the center of mass relative to the mobile platform (coincident with the cube's center).

Depending on the cube's size H_c in relation to H and H_{CoM}, different designs emerge. In the following examples, $H = 100\,mm$ and $H_{CoM} = 20\,mm$.

5.1 Small cube. When the cube size H_c is smaller than twice the height of the CoM H_{CoM} (8), the resulting design is shown in Figure 12.

$$H_c < 2H_{CoM} \tag{8}$$

This configuration is similar to that described in [11], although they do not explicitly identify it as a cubic configuration. Adjacent struts are parallel to each other, differing from the typical architecture where parallel struts are positioned opposite to each other.

This approach yields a compact architecture, but the small cube size may result in insufficient rotational stiffness.

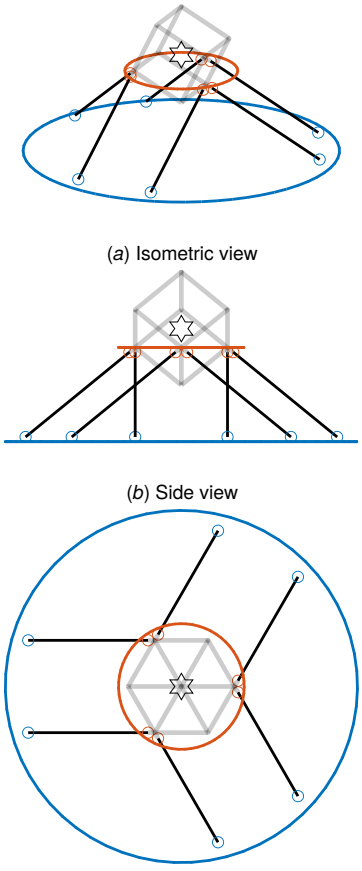

Figure 12 Cubic architecture with cube's center above the top platform. A cube height of 40mm is used.

5.2 Medium sized cube. Increasing the cube's size such that (9) is verified produces an architecture with intersecting struts (Figure 13).

$$2H_{CoM} < H_c < 2(H_{CoM} + H) \tag{9}$$

This configuration resembles the design proposed in [12], although their design is not strictly cubic.

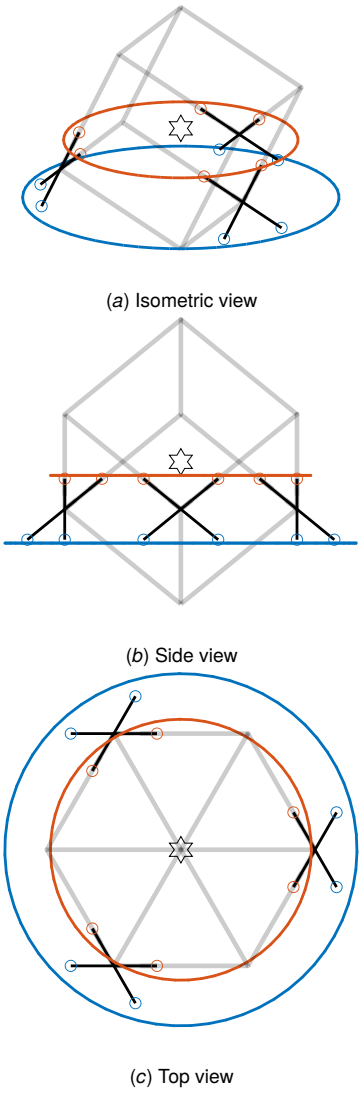

Figure 13 Cubic architecture with cube's center above the top platform. A cube height of 140mm is used.

5.3 Large cube. When the cube's height exceeds twice the sum of the platform height and CoM height (10), the architecture shown in Figure 14 is obtained.

$$2(H_{CoM} + H) < H_c \tag{10}$$

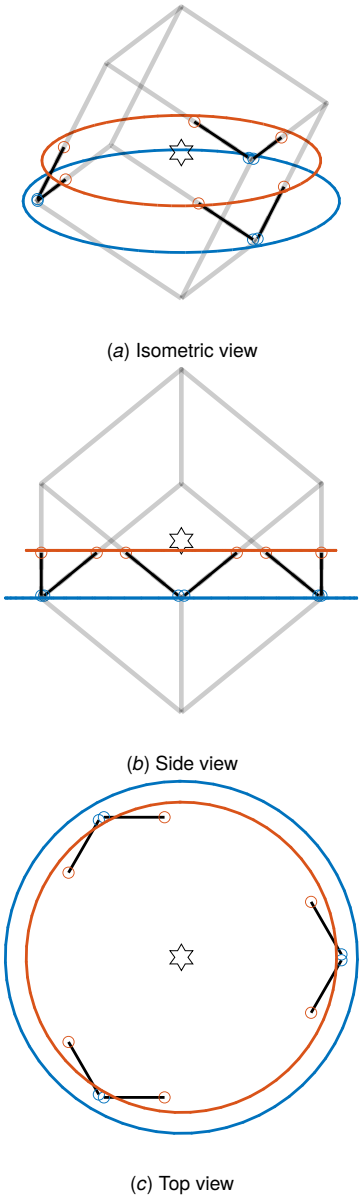

(*a*) Isometric view

(*b*) Side view

(*c*) Top view

Figure 14 Cubic architecture with cube's center above the top platform. A cube height of 240mm is used.

5.4 Platform size. For the proposed configuration, the top joints $\boldsymbol{b}_i$ (resp. the bottom joints $\boldsymbol{a}_i$) and are positioned on a circle with radius R_{b_i} (resp. R_{a_i}) described by Equation (11).

$$R_{b_i} = \sqrt{\frac{3}{2}H_c^2 + 2H_{CoM}^2} \tag{11a}$$

$$R_{a_i} = \sqrt{\frac{3}{2}H_c^2 + 2(H_{CoM} + H)^2} \tag{11b}$$

Since the rotational stiffness for the cubic architecture scales with the square of the cube's height (3), the cube's size can be determined based on rotational stiffness requirements. Subsequently, using Equation (11), the dimensions of the top and bottom platforms can be calculated.

Conclusion

The analysis of the cubic architecture for Stewart platforms yielded several important findings. While the cubic configuration provides uniform stiffness in the XYZ directions, it stiffness property becomes particularly advantageous when forces and torques are applied at the cube's center. Under these conditions, the stiffness matrix becomes diagonal, resulting in a decoupled Cartesian plant at low frequencies.

Regarding mobility, the translational capabilities of the cubic configuration exhibit uniformity along the directions of the orthogonal struts, rather than complete uniformity in the Cartesian space. This understanding refines the characterization of cubic architecture mobility commonly presented in literature.

The analysis of decentralized control in the frame of the struts revealed more nuanced results than expected. While cubic architectures are frequently associated with reduced coupling between actuators and sensors, this study showed that these benefits may be more subtle or context-dependent than commonly described. Under the conditions analyzed, the coupling characteristics of cubic and non-cubic configurations, in the frame of the struts, appeared similar.

Fully decoupled dynamics in the Cartesian frame can be achieved when the center of mass of the moving body coincides with the cube's center. However, this arrangement presents practical challenges, as the cube's center is traditionally located between the top and bottom platforms, making payload placement problematic for many applications.

To address this limitation, modified cubic architectures have been proposed with the cube's center positioned above the top platform. Three distinct configurations have been identified, each with different geometric arrangements but sharing the common characteristic that the cube's center is positioned above the top platform. This structural modification enables the alignment of the moving body's center of mass with the center of stiffness, resulting in beneficial decoupling properties in the Cartesian frame.

ASME Technical Publications provided the format specifications for the Journal of Mechanical Design, though they are not easy to reproduce. It is their commitment to ensuring quality figures in every issue of JMD that motivates this effort to have authors review the presentation of their figures.

Thanks go to D. E. Knuth and L. Lamport for developing the wonderful word processing software packages TEX and LATEX. We would like to thank Ken Sprott, Kirk van Katwyk, and Matt Campbell for fixing bugs in the ASME style file `asme2ej.cls`, and Geoff Shiflett for creating ASME bibliography stype file `asmems4.bst`.

References

[1] Stewart, D., 1965, "A platform with six degrees of freedom," *Proceedings of the institution of mechanical engineers,* **180**(1), pp. 371–386.

[2] Geng, Z. J., and Haynes, L. S., 1994, "Six degree-of-freedom active vibration control using the stewart platforms," *IEEE Transactions on Control Systems Technology,* **2**(1), pp. 45–53.

[3] Preumont, A., Horodinca, M., Romanescu, I., de Marneffe, B., Avraam, M., Deraemaeker, A., Bossens, F., and Abu Hanieh, A., 2007, "A six-axis single-stage active vibration isolator based on stewart platform," *Journal of Sound and Vibration,* **300**(3-5), pp. 644–661.

[4] Jafari, F., and McInroy, J. E., 2003, "Orthogonal gough-stewart platforms for micromanipulation," *IEEE Transactions on Robotics and Automation,* **19**(4), 8, pp. 595–603.

[5] Abu Hanieh, A., 2003, "Active isolation and damping of vibrations via stewart platform," PhD thesis, Université Libre de Bruxelles, Brussels, Belgium.

[6] Preumont, A., 2018, *Vibration Control of Active Structures - Fourth Edition* Solid Mechanics and Its Applications. Springer International Publishing.

[7] Thayer, D., Campbell, M., Vagners, J., and von Flotow, A., 2002, "Six-axis vibration isolation system using soft actuators and multiple sensors," *Journal of Spacecraft and Rockets,* **39**(2), pp. 206–212.

[8] McInroy, J. E., and Hamann, J. C., 2000, "Design and control of flexure jointed hexapods," *IEEE Transactions on Robotics and Automation,* **16**(4), pp. 372–381.
[9] Li, X., 2001, "Simultaneous, fault-tolerant vibration isolation and pointing control of flexure jointed hexapods," PhD thesis, University of Wyoming.
[10] McInroy, J. E., 1999, "Dynamic modeling of flexure jointed hexapods for control purposes," In Proceedings of the 1999 IEEE International Conference on Control Applications (Cat. No.99CH36328).
[11] Furutani, K., Suzuki, M., and Kudoh, R., 2004, "Nanometre-cutting machine using a stewart-platform parallel mechanism," *Measurement Science and Technology,* **15**(2), pp. 467–474.
[12] Yang, X., Wu, H., Chen, B., Kang, S., and Cheng, S., 2019, "Dynamic modeling and decoupled control of a flexible stewart platform for vibration isolation," *Journal of Sound and Vibration,* **439**, 1, pp. 398–412.